Dynamic Rheology and Morphology of Polylactide/ Organic Montmorillonite Nanocomposites

Biao Wang, Tong Wan, Wei Zeng

College of Material Science and Chemical Engineering, Tianjin University of Science and Technology, Tianjin 300457, China

Received 14 June 2010; accepted 5 November 2010
DOI 10.1002/app.33717
Published online 25 February 2011 in Wiley Online Library (wileyonlinelibrary.com).

ABSTRACT: The effects of organic montmorillonite (OMMT) on the rheological behaviors and phase morphology of polylactide (PLA) were investigated. The rheological behaviors of nanocomposites showed mainly dependence on both temperature and OMMT content. At low OMMT loading (1 wt %), the complex viscosities showed a Newtonian plateau in low frequency region at low temperatures and converted to a shear-thinning behaviors with increasing temperature. In comparison, at high OMMT loadings (above 5 wt %), strong shear-thinning behaviors were observed in the full range of frequencies and temperatures. The results demonstrated rheology of PLA/OMMT is highly sensitive to the nanofillers filled materials. A pseudo-solid-like behavior at long scale time in the hybrids with OMMT loading was higher than 5 wt %, this response was related to the formation of a network structure across the polymer matrix due to strong interactions of PLA and OMMT that confined the relaxation process of the macromolecules. X-ray diffraction and transmission electron microscopy indicated the nanocomposites at low OMMT loading were mainly exfoliated and intercalated nanocomposites were gradually formed with increasing OMMT loading. © 2011 Wiley Periodicals, Inc. J Appl Polym Sci 121: 1032–1039, 2011

Key words: PLA; montmorillonite; rheology; viscoelasticity; nanocomposite

INTRODUCTION

Polylactic acid (PLA) is one of linear aliphatic polyesters derived from 100% renewable resources, such as sweet corns and sugar beets. PLA is synthesized by either direct condensation of lactic acid or by the ring-opening polymerization of the cyclic lactide dimer. PLA has two enantiomeric forms (D and L) of lactic acid. Enantiomerically pure PLA is a semicrystalline polymer. PDLLA, which contains both D and L forms of lactic acid, is an amorphous polymer. PLA, possessed many physical characteristics, is suitable for replacing commodity polymers.[1] Its advantages are high strength, biocompatibility, thermoplastic fabricability, good crease-retention, grease and oil resistance, and excellent aroma barriers.[2–5]

Recently, one of particular commercial interest of PLA is developing PLA nanocomposites, which exhibit remarkably improved mechanical and various other properties as compared to those of virgin polymers.[6]

PLA is well suitable for sheet extrusion, film blowing, and fiber spinning, but it is only marginally acceptable for some other types of fabrication. The melt viscosity of PLA, typical of aliphatic polyester, is not very shear sensitive and the melt has relatively poor strength. To enhance the rheology of PLA for operations where shear sensitivity and melt strength are desirable, incorporating OMMT is employed in view of the much predominant properties of PLA.

It is well-known that there are two ideal types of nanostructures in Polymer/OMMT nanocomposites, intercalation, and exfoliation. The intercalated structure is formed when a few polymer molecules are inserted into the OMMT gallery and exfoliated structure is formed when the silicate layers are individually dispersed in Polymer matrix. However, real morphologies of PLA/OMMT nanocomposites often contain the two idealized microstructures.[7,8] Although all these structures often coexist in the Polymer/OMMT nanocomposites, it is believed that the remarkable mechanical, flammability, and barrier properties of these materials result from the large amount of the exfoliated silicate layers.[7,8]

In this article, Polylactide/organic montmorillonite nanocomposites were successfully prepared by melt-compounding technique and the effects of OMMT on the rheological behaviors and phase morphology of PLA were investigated. The main objective of this article is to relate the rheological

Correspondence to: B. Wang (wb22@tust.edu.cn).
Contract grant sponsor: The Foundation of Tianjin University of Science and Technology; contract grant number: 20090405.

behaviors of the PLA/OMMT nanocomposites with phase morphologies.

EXPERIMENTAL

Material and preparation of nanocomposites

PLA polymer 4060D, a product from NatureWorks® (registered trademark of Cargill Dow) was used in this article. This grade of NatureWorks® PLA is amorphous with weight average molecular weight of 1.4×10^5 and polydispersibility index of 1.5 as measured by GPC. The organic montmorillonite (OMMT; model: NB-901) was supplied by Huate Chemical (Zhejiang, China) and was modified by octadecylammonium ions.

PLA pellets and OMMT powder were dried in a vacuum oven at 50°C for 24 h to remove moisture prior to melt compounding process. PLA and OMMT were melt compounded in a Haake Polylab Rheomix 600p at 180°C and 30 rpm for 6 min till the torque reached constant. Neat PLA as a reference was processed in the Haake mixer under the same conditions for comparison. The film samples were prepared from the blends and neat PLA by heat pressing at 180°C. Some strands of the blends were placed in a compression mold to ensure a constant size ($90 \times 60 \times 0.7$ mm) and covered with aluminum foil sheets to prevent sticking to the press plates. This assembly was then placed between the press plates for 3 min without applying pressure, until the material was sufficiently melted, and then pressed for 2 min at a pressure of 10 MPa. The whole assembly with the press plates was then cool pressed for 3 min at a pressure of 10 MPa in air. The compression molded specimens were then stored in a desiccator awaiting analysis. The sample code was designated as neat PLA, PLAM1, PLAM5, and PLAM10 according to the mass ratio of PLA/OMMT: 100/0, 99/1, 95/5, and 90/10.

Characterization

Wide-angle X-ray diffraction (WAXD)

WAXD analysis were performed for OMMT powder, neat PLA, and PLA/OMMT nanocomposites using a Rigaku D/max 2500V/PC X-ray diffractometer (Cu K_α radiation $\lambda = 1.54056$ Å), operated at 50 kV and 250 mA. Scanning angle (2θ) ranged from 1° to 30° at the rate of 3°/min.

Transmission electron microscopy (TEM)

Ultrathin specimens (thickness in 50 nm) for TEM were cut using a Leica ultramicrotome with a diamond knife. The TEM micrographs were taken from JEM-1011 TEM under an accelerate voltage of 100 kV.

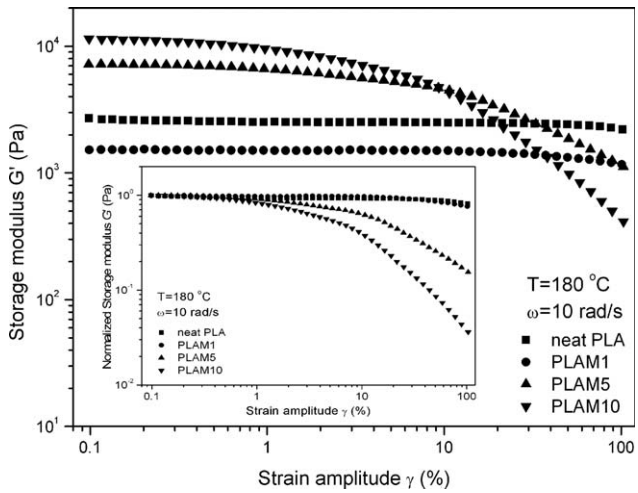

Figure 1 Strain amplitude dependence of storage modulus at a constant frequency of 10 rad/s at 180°C for neat PLA and 1, 5, 10 wt % composites.

Rheological test

Prior to rheological measurements, the compression-molded specimens were cut into the disks with 25 mm in diameter and dried at 50°C for 24 h. A strain-controlled rotational rheometer (Physica, MCR300, Austria) was employed to measure the viscoelastic response of PLA/OMMT nanocomposites. A pair of 25 mm parallel plates was used to carry out dynamic (oscillatory) tests with a fixed gap of 0.5 mm in the temperature range from 170 to 230°C under nitrogen atmosphere. Strain amplitude sweeps were performed at 1% in advance to assure that dynamic tests were in the linear viscoelastic range. Frequency range from 0.1 to 100 rad s^{-1} were applied for dynamic tests.

RESULTS AND DISCUSSION

Dynamic rheological properties

The transition from linear to nonlinear viscoelastic behavior, as manifested in dynamic oscillatory experiments (amplitude sweep), for neat PLA, PLAM1, PLAM5, and PLAM10 were shown in Figure 1. We focus on the storage modulus, as it is the most sensitive rheological function to the changes in the mesoscopic structure of hybrids. To compare and to elucidate the onset of shear thinning, the G' data shown in Figure 1 are normalized by the linear viscoelastic values at low shear strain amplitudes and shown in the insert. The normalized storage moduli exhibit the expected shear-thinning behavior with increasing OMMT loading, namely, the critical strain amplitude for the transition were decreased with increasing OMMT loading. Furthermore, the storage modulus of nanocomposites increase with

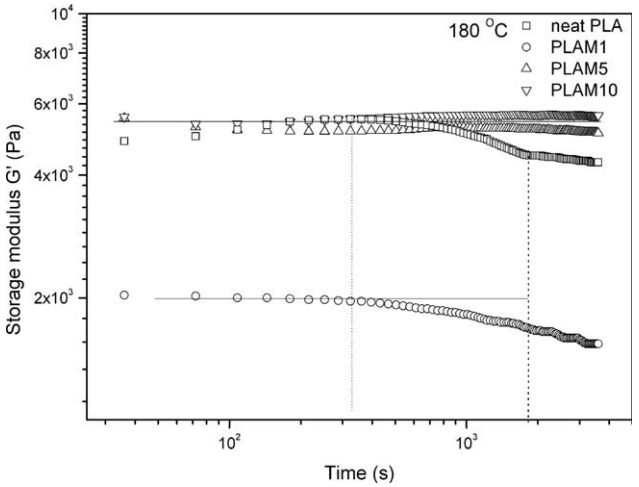

Figure 2 Time sweep curves for neat PLA and PLA/OMMT nanocomposites at 180°C.

OMMT loading as expected except for PLAM1, which has lower storage modulus than neat PLA.

The silicate layers and tactoids (collection of intercalated silicate layers that are locally correlated) are randomly organized under quiescent state. However, the tactoids gradually oriented aligned parallel to the flow direction under shear amplitude. The orientation of anisotropic silicate layers under oscillatory shear was demonstrated using X-ray diffraction (XRD), TEM, and rheology evaluations.[9–12] X-ray measurements showed that the silicate layers were oriented in the direction of the shear and leaded to a dramatic change in linear viscoelastic behavior at low frequency from liquid-like to almost solid-like (detailed discussion later). Furthermore, it is expected that in the quiescent state, with increasing silicate loading a larger fraction of the tactoids would be hydrodynamically hindered and caused gradually increase in the filler-filler interaction.[13]

Additionally, with increasing OMMT loading, the ease extent to which the filler structure can be altered by flow is considerably enhanced primarily owing to increased filler-filler interactions. It is easily understood that the threshold of strain amplitude for the onset of shear thinning decreases with increasing OMMT loading, and the shear-thinning dependence of strain amplitude is improved at higher OMMT loadings.

Figure 2 shows time sweep results within the linear viscoelastic regime for neat PLA and PLA/OMMT nanocomposites. The storage modulus G' as a function of time was presented for nanocomposites with various amounts of OMMT. Neat PLA exhibits a quick decreasing G' as a function of time for about half of an hour, and then continues to decrease in lesser extent. The value of G' for PLAM1 is below that of neat PLA within whole studied time range which is in accordance with previous strain sweep result. For PLAM5 and PLAM10, it shows that both the G' values remain constant though the difference of two value size. It is concluded that adding over 5 wt % OMMT to PLA matrix a stable viscoelastic response can be obtained for about 1 h at least.

The complex viscosities of the nanocomposites with various OMMT loading were presented in Figure 3(a). It is interesting that the inclusion of low OMMT loading (1 wt %) lower the complex viscosity of PLA matrix. Li has reported that apparent melt viscosity of PEG/OMMT/PP composite with low OMMT loading (< 5 wt %) is much lower than that of pure PP at low shear rates and the role of lubricant carrier of OMMT is responsible for the reduction viscosity.[14] In the article, this may result from rotating more freely and orientation of silicate layers when they were suffered to shear for the nanocomposite

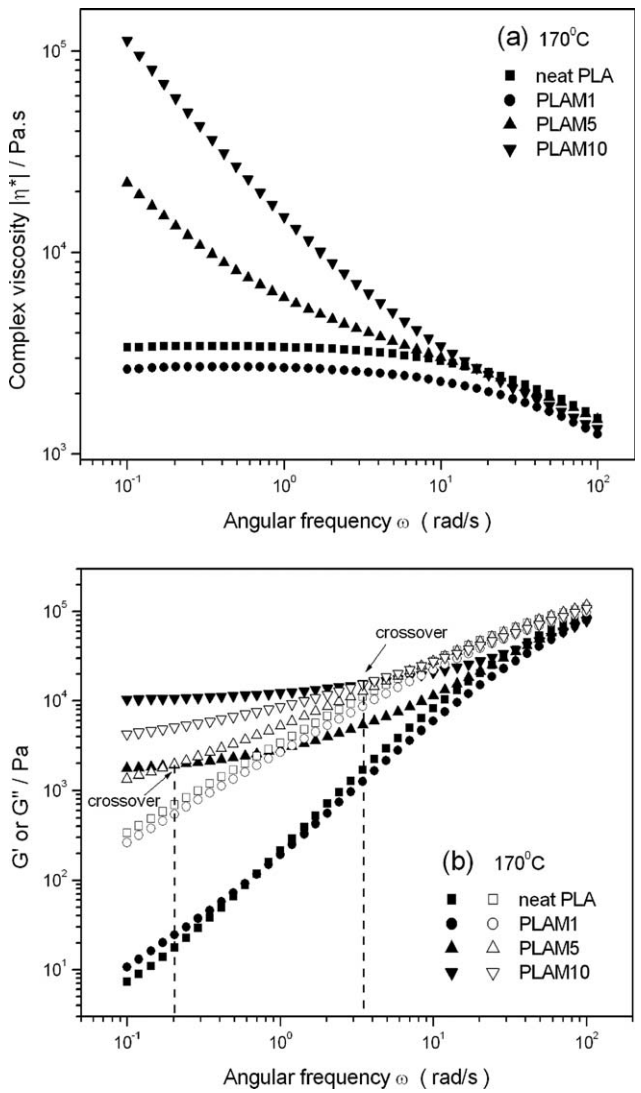

Figure 3 Complex viscosity as a function of frequency for neat PLA and PLA/OMMT nanocomposites at 170°C (a). Storage modulus (solid symbol) and loss modulus (open symbol) as a function of frequency for neat PLA and PLA/OMMT nanocomposites at 170°C (b).

with lower silicate loading due to the weaker filler-filler interaction.[13] Moreover, beyond a critical volume fraction, the tactiods and individual layers are incapable of rotating freely and are prevented from complete relaxation when subjected to shear. This incomplete relaxation leads to the presence of the pseudo-solid-like behavior observed in both intercalated and exfoliated nanocomposites.[10] Therefore, the reduction storage modulus of PLAM1 as shown in Figure 1 and 2 is related to the lower complex viscosity in view of equation $G' = \omega\eta''=\omega|\eta^*|\cos\delta$, where η'' is viscous dynamic viscosity and δ is phase angle.

Liu et al reported that the exfoliated silicate layers were formed at low clay loadings (less than 4 wt %) when they studied the nylon 11/organoclay nanocomposites.[15] Therefore, we predicted that the silicate layers mainly achieved the exfoliated state for PLAM1 and this is supported by the later WAXD and TEM result.

The PLA matrix and the PLAM1 displayed a pseudo-Newtonian behavior at low angular frequency range, while other samples showed a higher complex viscosity and a more pronounced shear thinning behavior with the increase of OMMT loading. For example, a linear increase was observed with decreasing frequency for the nanocomposite containing 10 wt % OMMT. Shear thinning pseudo-non-Newtonian behavior was observed in some conventional thermoplastic composites: some studies on dispersed flow of particulate-filled polymers, containing high percentage of fillers (glass spheres, barium sulfate, calcium carbonate powder), demonstrated that the dynamic viscosities increased with the filler concentration and, beyond a critical concentration, showed a divergence at low frequencies indicating a structure change of the network formed by the particles.[16] The exact concentration at which a continuous structure network was formed depending on the nature of the filler, its size, and the interactions between the filler and the suspending medium.

It was clear in the Figure 3(b) that neat PLA exhibited the pure liquid-like relaxation behavior and G'' dominated over G' at all studied frequency range, implying viscous characteristic excelled the elasticity for neat PLA at melt state. Additionally, it seemed that there was a crossover at about 100 rad/s between storage modulus and loss modulus. The similar phenomenon was also observed for nanocomposites of high OMMT loadings (e.g., 5 wt % and 10 wt %). The corresponding frequency ω_{cro} at crossover point was 0.203 rad/s and 3.46 rad/s for PLAM5 and PLAM10, respectively. It was evident that PLAM10 exhibited the elasticity more quickly than PLAM5 at 170°C owing to the intersection locating in higher frequency (shorter time). Further, this crossover corresponded to a transition in viscoelastic behavior dominated by relaxation of unentangled polymer chains to that was dominated by layered silicate superstructure. Therefore, the introduction of layered silicate apparently enhanced the elasticity property of PLA matrix, especially for composites of high silicate loadings.

At 170°C and low frequencies, PLA molecular chains were fully relaxed and exhibited typical homopolymer-like terminal behavior with scaling properties of approximately $G' \sim \omega^2$ and $G'' \sim \omega$ as shown in Figure 3(b) (this power law may vary owing to the polydispersity of polymer chains). However, this terminal behavior disappeared when OMMT loading was higher than 5 wt %, and the dependence of G' and G'' on ω at low frequency was weak. The incorporation of OMMT to PLA dramatically increased the G' and G'', particularly at low frequencies and the developed plateaus of G' and G'' were detected. This effect was more pronounced in G' than that in G''. The frequency dependence of G'' showed a similar trend. The structure network formed in nanocomposites was emphasized by the behavior of the storage modulus G', extremely sensitive to morphological state. The almost independence of G' on ω and a divergence of complex viscosity at low frequency when the OMMT loading was higher than 5 wt %, indicated a transition from liquid-like to solid-like viscoelastic behavior in the composite. This nonterminal low frequency behavior was a characteristic for the formation of clay network-like structures that restrained the long-range motion of polymer chains and can be attributed to the percolation of the fillers.[17] Thus, large-scale polymer relaxations in composites were effectively restrained by the presence of OMMT. Similar rheological behaviors were observed in polymer composites containing clays or MWNTs.[18–23]

At high frequencies, the characteristic of processing behavior, the effect of OMMT on the rheological behavior was relatively weak. Thus, the composites containing OMMT were expected to exhibit the same processing behavior as the neat polymer in practical applications almost. This behavior suggested that the OMMT did not significantly influence the short-range dynamics of the PLA chains.

In addition, the influence of temperature on the complex viscosity $|\eta^*|$ was investigated in the range of between 170 and 230°C. Figure 4 showed the complex viscosity of neat PLA and PLAM1 at four different temperatures. Neat PLA presented the characteristic of Newtonian liquid at low frequency and its $|\eta^*|$ was strongly sensitive to temperature. From 170°C to 230°C, $|\eta^*|$ of Neat PLA reduced from 3410 to 230 Pa·s at 1 rad/s as shown in Table I and Figure 4. Furthermore, the onset frequency of shear-thinning gradually increased from 1.7 to 20.3 rad/s when the temperature was raised from 170 to 230°C.

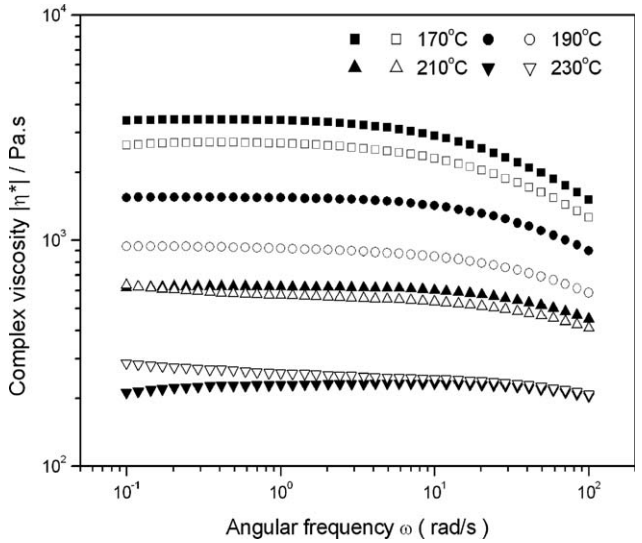

Figure 4 Effect of temperature on complex viscosity for neat PLA (solid symbol) and PLAM1 (open symbol) at temperature of 170, 190, 210, and 230°C.

It was clear that incorporating OMMT into PLA enhanced the stability of PLA, particularly at high temperatures. The complex viscosities of PLAM1 were lower than those of neat PLA both at 170 and 190°C and the difference of complex viscosities of PLAM1 between 170 and 190°C was lower than that of neat PLA, suggesting that PLA softened more rapidly and had a better processing behavior below 190°C than PLAM1. However, with increasing temperature the value of viscosity of PLAM1 approached (51 Pa·s at 210°C) and even exceeded (−29 Pa·s at 230°C) that of neat PLA as shown in Table I. Moreover, the difference of complex viscosities of PLAM1 (315 Pa·s) at both higher temperatures was closer than that of neat PLA (395 Pa·s), implying that neat PLA softened more rapidly and had less stability than PLAM1 at high temperature. Especially, between 190 and 210°C, the value change of complex viscosity for PLAM1 (344 Pa·s) was much lower than that of neat PLA (915 Pa·s), suggesting that the stability of PLAM1 was best between 190 and 210°C. Moreover, the Newtonian plateau of complex viscosity for PLAM1 at low frequency was displaced by shear-thinning curves when the temperature was raised to 210°C.

In addition, the validity of time-temperature superposition principal (TTS) was checked by plotting the phase angle δ (atan G''/G') versus the absolute value of the complex modulus $|G^*|$ ($(G'^2+G''^2)^{1/2}$) (van Gurp's plot).[24] TTS was fulfilled if the un-shifted isotherms fall on one curve. Figure 5 showed the corresponding data of neat PLA and PLA/OMMT composites. It was apparent in the figure that TTS did hold in the case of neat PLA because the isotherms did merge into a common curve. The data for the nanocomposite with 1 wt % OMMT exhibited minor failures from TTS, with divarication at low complex modulus. Further, the nanocomposites with 5 and 10 wt % OMMT did not follow the TTS at all complex modulus. With increasing the OMMT loading from 1 to 10 wt %, the materials became more and more elastic. The smaller δ values of composites at small moduli revealed an even higher elasticity in compare to neat PLA.

A unique type of van Gurp's curve is typical for linear samples. This type of curve is characterized by one minimum and one inflection point. The locations of these points and thus the shape of the curve are correlated to the plateau modulus, to the molecular weight, and, especially, to the polydispersity. A typical linear polymer has a unique course of curve like that moving from high to low modulus value of the phase angle δ drops, passes a minimum, rises again, moves through an inflection point and finally approaches its value of 90°. This characteristic curvature is found for amorphous polymers such as polystyrene.[25] For crystalline polymers like polyethylene only the part on the left side of the minimum can be monitored by melt rheology, since crystallization occurs at the low temperatures that are necessary to reach the minimum region.

For our samples, only the sample PLAM10 exhibited this characteristic curve at higher temperature (230°C) as shown in Figure 5. Apparently, the horizontal positions of the minimum scattered around 6×10^3 Pa, which was the value of the PLAM10 plateau modulus G_N^o. This finding can be reasoned by a mathematical consideration. The plateau modulus is defined by eq. (1):

$$G_N^o = G'(\omega|_{\tan\delta \text{ at min}}) \quad (1)$$

This definition can be expressed in term of $|G^*(\delta)|$: $G_N^o = \lim_{\delta\to 0}|G^*(\delta)|$ when $\delta\to 0$, then

TABLE I
The Complex Viscosity of Neat PLA and PLAM1 Nanocomposite at Different Temperatures

Sample	170°C	190°C	210°C	230°C	$\lvert\eta^*\rvert_{170}$-$\lvert\eta^*\rvert_{190}$	$\lvert\eta^*\rvert_{190}$-$\lvert\eta^*\rvert_{210}$	$\lvert\eta^*\rvert_{210}$-$\lvert\eta^*\rvert_{230}$
Neat PLA	3410	1540	625	230	1870	915	395
PLAM1	2690	918	574	259	1772	344	315
$\lvert\eta^*\rvert_{PLA}$-$\lvert\eta^*\rvert_{PLAM1}$	720	622	51	−29	–	–	–

The dynamic angular frequency ω is set at 1 rad/s and the unit of complex viscosity is Pa·s.

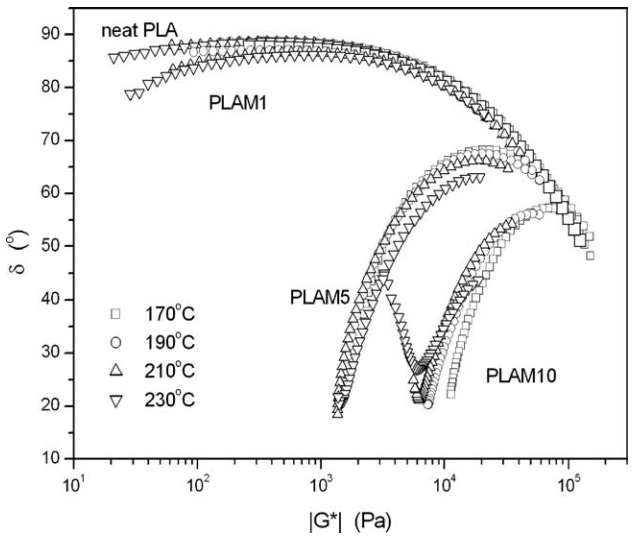

Figure 5 van Gurp plots of neat PLA and three nanocomposites with different OMMT loading.

tanδ→0 (that is also the minimum), G' dominates over G'' and finally disappears such that $|G^*|$ approaches G'. Therefore, $|G^*|$ in the minimum equals the plateau modulus. Keeping this in mind, it can be stated that the minimum in the van Gurp's plot is associated with the plateau modulus G_N^o and the lower this minimum is located on the vertical axis, the more accurately does the $|G^*|$ value in the minimum correspond to the plateau modulus G_N^o.

Structure and morphology

The structure of the nanocomposites was typically established by using WAXD patterns and TEM observations. WAXD allowed a direct evidence of the intercalation of polymer chains into the silicate layers, whereas TEM offered a qualitative understanding of the internal structure through direct visualization. WAXD patterns of OMMT powder and PLA/OMMT nanocomposites with various OMMT loadings in the range $2\theta = 1.8^\circ - 9.0^\circ$ were presented in Figure 6. The WAXD pattern of the organic montmorillonite showed a diffraction peak of at about $2\theta = 4.48^\circ$, corresponding to a basal spacing of 1.97 nm. As a result, after incorporating with PLA by melt compounding the d-spacing of OMMT increased from 1.97 to 3.45 nm, which was obtained from the observed peaks of the angular position (2θ) according to the Bragg formula ($n\lambda = 2d \sin\theta$). This change in d-spacing indicated that PLA chains were intercalated into the OMMT interlayers.[26] Meanwhile, the maximum peak intensities of PLAM1, PLAM5, and PLAM10 located at about the same angular positions, suggesting that d-spacing for the PLA/OMMT nanocomposites was independent of the OMMT loading. This result was agreement with the previous reported literatures.[26,27] In spite of the absence of the basal plane, a small peak in the small-angle region was usually observed in WXRD patterns for the obtained nanocomposites with various OMMT loading, probably indicating the formation of exfoliated, intercalated or partially exfoliated/partially intercalated structures. Further, it was distinctly that the peak intensity of PLAM5 at small-angle region was larger than those of PLAM1 and PLAM10, suggesting that more orientation of silicate layers was formed in the PLAM5 nanocomposites. Hence, it seemed reasonable that Kojima et al. used the peak intensity together with the interlayer spacing to characterize the relative proportion of exfoliated and intercalated species with the nanofiller content.[28] For the studied PLA/OMMT nanocomposites, it was likely that the exfoliated structure was the dominant population when the concentration was below 5 wt %; and above it, the intercalated hybrid gradually dominated; and for 5 wt %, the exfoliated structure with partially ordering structure was probably formed.[29] In addition, for the nanocomposites with high OMMT loading (e.g., 10 wt %), though the intercalated structure was dominant there were more aggregative silicate layers without intercalated PLA chains in the matrix. These speculations were further confirmed by TEM observation as illustrated in Figure 7. TEM images (a), (b), and (c) showed typical but various OMMT dispersions for PLA nanocomposites containing organic montmorillonite of 1, 5, and 10 wt %, respectively. It can be seen that the silicate plates (dark lines) or silicate bundles (dark area) were homogeneously dispersed in the polymer matrix in all three cases. Clearly, the PLAM1 (at low OMMT loading, 1 wt %) was a typical characteristic of

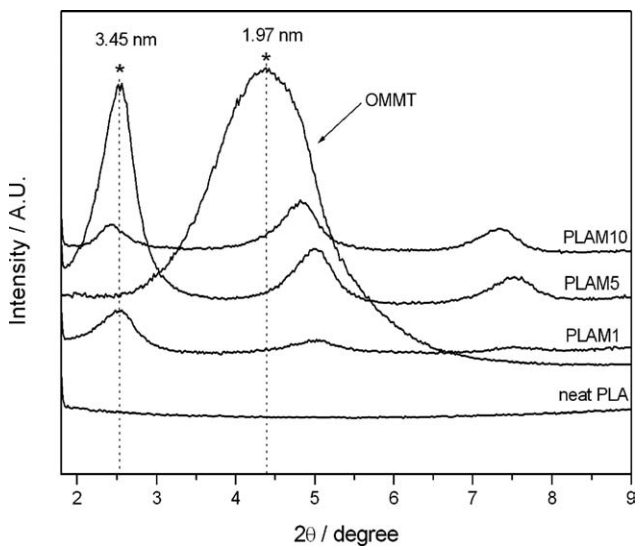

Figure 6 The WAXD patterns of organically modified montmorillonite powder, neat PLA and the nanocomposites with different OMMT loading.

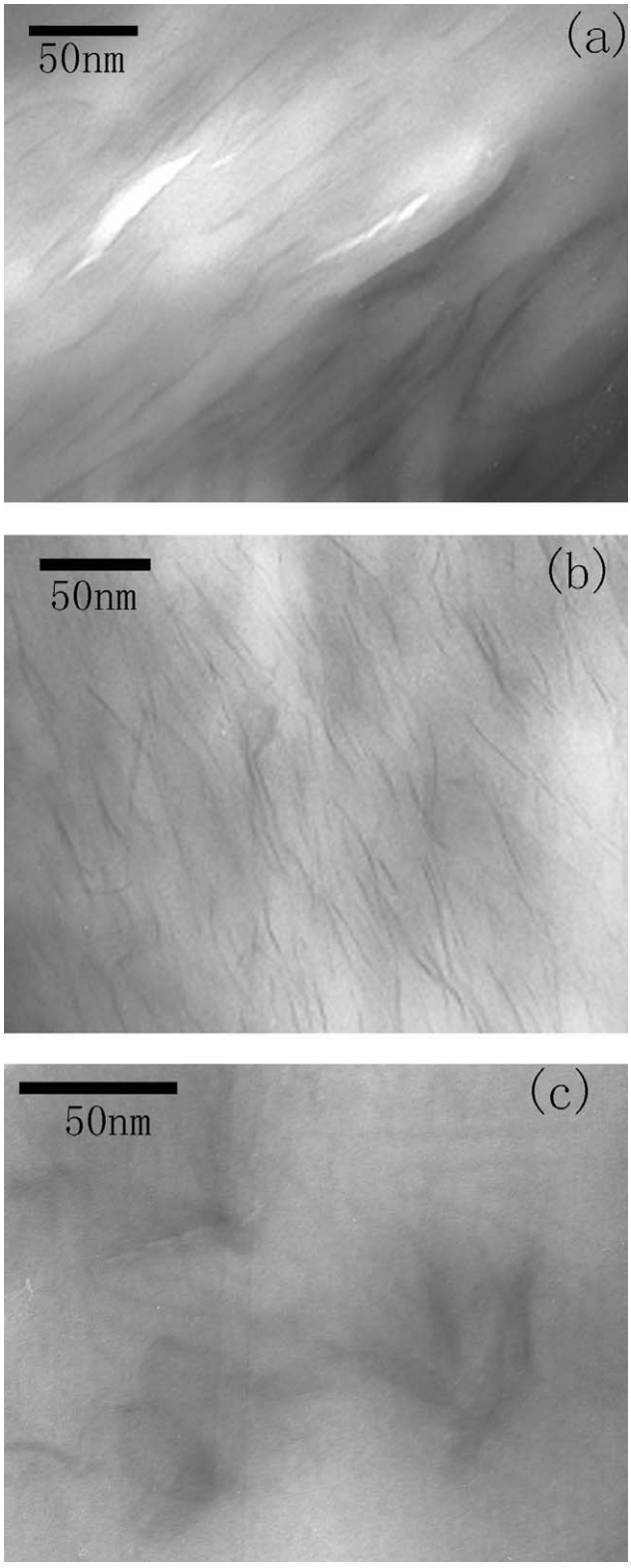

Figure 7 The TEM images of PLA/OMMT nanocomposite. PLAM1 (a), PLAM5 (b), and PLAM10 (c). The dark lines or area are silicate layers and the white matrix is polymer.

disordered and exfoliated OMMT nanostructure and silicate layers rotated and orientated more freely when they were suffered the shear due to the weaker filler-filler interaction. Thus, the PLAM1 displayed a pseudo-Newtonian behavior at low frequency range as does neat PLA in Figure 3. The more ordered and exfoliated OMMT layers were observed for the PLAM5 (5 wt % OMMT loading), which observably restrained the motion of polymer chains and led to a transition from liquid-like to solid-like viscoelastic behavior in composites. Whereas the PLAM10 (at high OMMT loading, 10 wt %) was typically ordered intercalated OMMT layers (dark area) morphology with some aggregative OMMT (darker area) and showed a higher complex viscosity and a more pronounced shear thinning behavior as indicated in Figure 3.

It should also be noted that, in practice, it is difficult to get fully exfoliated or fully intercalated polymer/OMMT nanocomposites at higher OMMT loadings, especially by the melt intercalation approach. The relative fraction of intercalation/exfoliation usually increased with increasing the OMMT loadings. Moreover, the OMMT agglomeration was usually inevitable to some extent at high OMMT loading (e.g., 10 wt %). In addition, diverse nanoscale morphologies of OMMT were usually observed by TEM.

CONCLUSIONS

Nanocomposites comprising of PLA and organic montmorillonite were prepared by melt-compound technique. The rheological behavior of nanocomposites showed dependence on both temperature and OMMT loadings. For the polymer and the nanocomposite of low OMMT loadings (1 wt %), the complex viscosity showed a Newtonian plateau in low frequencies at low temperatures. The nanocomposites exhibited strong shear-thinning behavior and nonterminal viscoelastic behavior at high temperature or high loadings of OMMT. The dynamic moduli measurements suggested the presence of pseudo-solid-like behavior for composites with OMMT loadings in excess of 5 wt %. The time sweeps showed that the stability of PLA matrix was improved by incorporating the more than 5 wt % OMMT loadings and TEM showed that the exfoliated nanocomposites was formed at low OMMT loadings (less than 5 wt %) and a mixture of exfoliated and intercalated nanocomposites was obtained at higher OMMT loadings.

References

1. Vert, M.; Schwarch, G.; Coudane, J. J Macromol Sci Pure Appl Chem 1995, A32, 787.
2. Lunt, J. Polym Degrad Stab 1998, 59, 145.
3. Wehrenberg, R. H. Mater Eng 1981, 94, 63.
4. Drumright, R. E.; Gruber, P. R.; Henton, D. E. Adv Mater 2000, 12, 1841.
5. Lipinsky, E. S.; Sinclair, R. G. Chem Eng Prog 1986, 82, 26.
6. Biswas, M.; Sinha Ray S. Adv Polym Sci 2001, 155, 167.

7. Chen, G. X.; Kim, H. S.; Shim, J. H.; Yoon, J. S. Macromolecules 2005, 38, 3738.
8. Chen, G. X.; Yoon, J. S. Clay Macromol Rapid Commun 2005, 26, 899.
9. Giannelis, E. P.; Krishnamoorti, R.; Manias, E. Adv Polym Sci 1999, 138, 107.
10. Ren, J.; Silva, A. S.; Krishnamoorti, R. Linear Macromol 2000, 33, 3739.
11. Krishnamoorti, R.; Giannelis, E. P. Macromolecules 1997, 30, 4097.
12. Krishnamoorti, R.; Vaia, R. A.; Giannelis, E. P. Chem Mater 1996, 8, 1728.
13. Galgali, G.; Ramesh, C.; Lele, A. Macromolecules 2001, 34852.
14. Zhu, S. P.; Chen, J. Y.; Li, H. L. Polym Bull 2009, 63, 245.
15. Liu, T. X.; Lim, K. P.; Tjiu, W. C.; Pramoda, K. P.; Chen, Z. K. Polymer 2003, 44, 3529.
16. Krishnamoorti, R.; Ren, J.; Silva, A. S. J Chem Phys 2001, 114, 4968.
17. Shenoy, A. V. Rheology of filled polymer systems; Kluwer Academic Publishers: London 1999; 243.
18. Sohn, J. I.; Lee, C. H.; Lim, S. T.; Kim, T. H.; Choi, H. J.; Jhon, M. S. J Mater Sci 2003, 38, 1849.
19. Gu, S. Y.; Ren, J.; Wang, Q. F. J Appl Polym Sci 2004, 91, 2427.
20. Meincke, O.; Hoffmann, B.; Dietrich, C.; Friedrich, C. Macromol Chem Phys 2003, 204, 823.
21. Du, F.; Scogna, R. C.; Zhou, W.; Brand, S.; Fischer, J. F.; Winey, K. I. Macromolecules 2004, 37, 9048.
22. Seo, M. K.; Park, S. J Chem Phys Lett 2004, 395, 44.
23. Pötschke, P.; Mahmoud, A. G.; Alig, I.; Dudkin, S.; Lellinger, D. Polymer 2004, 45, 8863.
24. van Gurp, M.; Palmen, J. Rhel Bull 1998, 67, 5.
25. Trinkle, S.; Friedrich, C. Rheol Acta 2001, 40, 322.
26. Hyun, Y. H.; Lim, S. T.; Choi, H. J.; Jhon, M. S. Macromolecules 2001, 34, 8084.
27. Zhu, J.; Wilkie, C. A. Polym Int 2000, 49, 1158.
28. Kojima, Y.; Usuki, A.; Kawasumi, M.; Okada, A.; Kurauchi, T.; Kamigaito, O. J Polym Sci Part A: Polym Chem 1993, 31, 1755.
29. Kickelbick, G. Prog Polym Sci 2003, 28, 83.